EEET ECOLOGICAL ENGINEERING & ENVIRONMENTAL TECHNOLOGY

Ecological Engineering & Environmental Technology, 2026, 27(8), 177–191
https://doi.org/10.12912/27197050/225247
ISSN 2719–7050, License CC-BY 4.0

Received: 2026.06.09
Accepted: 2026.07.10
Published: 2026.08.01

Landslide susceptibility mapping and model validation using AHP and GIS techniques: A case study of Jerash, Jordan

Razan AlFukaha[1*], Mohammad Alharahsheh[2], Majed Ibrahim[2,3], Mohamed Tayebi[1]

[1] Faculty of Sciences, Department of Geology, Université Ibn Tofail, Kénitra 14000, Morocco
[2] Department of Geographic Information Systems and Remote Sensing, Faculty of Earth and Environmental Sciences, Al Al-Bayt University, Al Mafraq, Jordan
[3] Faculty of Technical Education, Al Al-Bayt University, Al Mafraq, Jordan
* Corresponding author's e-mail: razanalfoqahaa@gmail.com

ABSTRACT

Landslides are a major geohazard in northern Jordan, especially in the Jerash region, where complex geological conditions, steep terrain, and increased human activity contribute to slope instability. The goal of this study is to assess landslide risk in the Jerash area using an integrated geographic information system (GIS) and analytic hierarchy process (AHP) method. Seven conditioning factors were selected based on area features, data availability, and previous research: slope, elevation, aspect, lithology, soil texture, land use/land cover (LULC), and rainfall. These parameters were weighted using AHP pairwise comparisons, yielding a consistency ratio of 0.05, indicating satisfactory reliability of the expert judgments. Then, the weighted thematic layers were combined in a GIS environment to create a landslide susceptibility map divided into low, moderate, and high susceptibility zones. The findings show that slope is important factor in determining landslide incidence in the research area, followed by soil texture and lithology. Areas with steep slopes, clay-rich soils, weak lithological units, heavy agricultural activity, and high rainfall are moderately to highly susceptible to landslides. Spatial validation against documented landslide locations shows a substantial correlation between observed events and anticipated high-susceptibility zones, validating the robustness of the proposed model. The created susceptibility map is useful for land use planning, infrastructure development, and catastrophe risk reduction measures in the Jerash region. Overall, this study demonstrates the usefulness of the GIS-AHP framework for landslide susceptibility evaluation in data-scarce, semi-arid environments and supports its use for long-term hazard management in northern Jordan.

Keywords: analytical hierarchy process, geographic information system, Jordan, landslide susceptibility, remote sensing.

INTRODUCTION

Landslides are among the natural disasters that inflict the greatest loss of life and property worldwide (Aydın et al., 2022). They refer to the gravitational descent of earth materials, including weathered rock, rock, soil, and debris. The primary causes of landslides include intense precipitation, snowmelt, geological factors, seismic activity, environmental conditions, anthropogenic activities, construction, deforestation, and mining (Demirel et al., 2025). A multitude of factors, varying in significance, might precipitate a landslide. These factors include construction activities, slope angle, slope aspect, slope curvature, proximity to faults, climatic conditions, and land cover, among others. Depending on the region, certain factors may be more or less important than others (Noorollahi et al., 2018).

Numerous landslides have transpired in Jordan during the past few decades. The majority of significant landslides have transpired along the Amman–Jerash–Irbid highway (AJIH), particularly during winter; numerous previous studies have identified various forms of slope failure in this area, including rockslides, rockfalls, slumping, and earth flows (Al-Rawabdeh et al., 2024). Landslide events in this region have increased significantly due to rapid climate change, high rainfall, and heightened human pressure. Landslides may be triggered by external or internal agents, such as slope steepening, removal of support from the slope, the addition of water or moisture in various forms, and the presence of fundamentally weak materials (Kanwal et al., 2017). Different factors, such as earthquakes, precipitation, and erosion, can also trigger landslides, posing a danger to people, industry, property, and highways, and causing massive damage (Ahmed et al., 2014). As a result, landslide susceptibility mapping is a crucial stage before landslide assessment, planning, management, and disaster mitigation. Identification and careful assessment of this underestimated threat are required for effective reduction of landslide hazard through disaster mitigation planning and development methods.

Recent research has established methods to quantify landslide vulnerability, demonstrating a rise from natural processes in past several decades (Althuwaynee and Pradhan 2016; Shahabi et al. 2015). These works on landslide susceptibility mapping have employed both deterministic models and probabilistic methodologies, considering whether future environmental conditions will satisfy the criteria for a landslide, as established by prior occurrences (El Jazouli et al. 2019). Qualitative approaches rely on the opinions of individual or group experts. Experts use inventory and historical data to evaluate landslides, identify underlying causes, and locate places with similar geological and geomorphological characteristics. The analytic hierarchy process (AHP) and other qualitative approaches may turn semi-quantitative through ranking and weighting (Ayalew et al. 2005; Saaty 1977; Barredo et al. 2000; Yalcin 2008).

The AHP is a measurement method used to address both quantitative and intangible criteria and has been implemented in various domains, including decision theory and conflict resolution (Vargas, 1990). This method disaggregates each layer used in landslide susceptibility zoning into smaller components, which are subsequently weighted by their significance, culminating in the assembly of the prepared layers into the final map. It is widely known that it has three components which are decomposition, comparative assessment, and synthesis of priorities (Malczewski, 1999). In this approach, the weight of each layer is contingent upon the expert's assessment; hence, the greater the accuracy of the judgment, the more congruent the resultant map is with reality (Moradi et al. 2012). Researchers have utilized several variants of the AHP technique to successfully analyze landslide susceptibility. Kumar and Anbalagan (2016) applied the AHP to landslide susceptibility mapping (LSM) in the Tehri reservoir rim region of Uttarakhand, India, achieving approximately 79% predictive accuracy by integrating multiple causative factors within a geographic information system (GIS) environment. Chen et al. (2016) employed AHP in combination with certain factor (CF) models to generate landslide susceptibility maps for a study area in China, considering conditioning factors including slope degree/aspect, altitude, plan curvature, geomorphology, distances from faults and rivers, and precipitation, and reporting an AHP model accuracy of approximately 78% in delineating susceptible zones. Recent studies have reaffirmed the relevance of the AHP approach in landslide susceptibility mapping. Liu et al. (2024) used the AHP model to produce a landslide susceptibility zonation map for the Great Xi'an Region in China, incorporating various conditioning factors such as elevation, slope, lithology, land use, and drainage density. Their findings indicated that regions identified as having high and very high vulnerability accounted for the bulk of documented landslide occurrences, thereby validating the efficacy of the AHP methodology. Likewise, Singh et al. (2024) performed a GIS-based assessment of landslide susceptibility in the Beas River Basin of the north-western Himalaya utilizing the AHP approach. Their findings indicated a strong correspondence between observed landslides and high-susceptibility zones, highlighting the effectiveness of AHP in mountainous terrains when supported by appropriate spatial datasets and validation techniques.

As a result, landslide susceptibility mapping is crucial for improving hazard and risk management in Jordan, particularly given the intricate interplay among geological, geomorphological, and soil factors influencing slope stability. Several studies in Jordan used remote sensing (RS), GIS, and statistical/machine learning techniques to assess and map landslide susceptibility. For example, Awawdeh et al. (2018) used a weighted overlay GIS-based method to create a landslide susceptibility map for northern Jordan and the Jerash-Amman corridor, highlighting zones of high to low susceptibility and identifying key controlling factors such as lithology, drainage, and road cuts. More recently, Al-Rawabdeh et al. (2023) created a landslide hazard zonation map for the Amman-Jerash-Irbid Highway by combining GIS and the fuzzy analytical hierarchy process (FAHP), testing the susceptibility classes against documented landslide inventory. Despite these efforts, there remains a lack of comprehensive landslide research in many parts of northern Jordan, including detailed susceptibility assessments tailored to the Jerash region, underscoring the ongoing need for more localized studies using integrated GIS-RS and quantitative modeling approaches.

Although landslide susceptibility has been identified for the Jordanian region through various studies, there is still a need for a localized model for the Jerash region. This is particularly true because the existing models might not account for the most significant parameters that affect the semi-arid region. Moreover, the validation process might not have been sufficiently accurate for the model's predictions. This research will fill the gap by designing an AHP-GIS model that can provide a reliable susceptibility map for the Jerash region.

This research aims to develop a landslide susceptibility map for the Jerash region by combining geospatial data with AHP and GIS architecture. They have proven effective for examining a wide range of modeling criteria. This study used a hybrid set of topographic, geological, and geomorphological factors to holistically assess landslide vulnerability. This model included criteria into a systematic multi-criteria decision-making (MCDM) framework. It improves model precision by leveraging complex spatial correlations and validation approaches, such as a validation model. This study strengthens the methodological framework for assessing landslide hazards in data-scarce, semi-arid environments. Landslides in the Jerash area are mostly influenced by internal variables such as the region's geological, geomorphological, and soil properties. The presence of eroded rock formations and soil types with poor shear strength makes slopes more prone to failure. This inherent instability is exacerbated by extrinsic factors, such as heavy precipitation and anthropogenic activities, including road construction and land-use changes, which together exert additional loads on slopes and trigger landslides.

STUDY AREA

The study area is located in the southern region of Jordan, Middle East, and is geographically 52 km north of Amman city. It is bounded by the coordinates 32°13 to 32° 28N and 35° 85 to 35° 91E, as shown in Figure 1. It encompasses roughly 420 km² and features a severe landscape with elevations ranging from 2 m to 1.229 m above sea level. These altitude fluctuations result in steep slopes that are frequently subject to geomorphological processes, including landslides and erosion (Abed et al., 2022). According to local statistics, the population in Jerash city is around 262,100 capita, which corresponds to a population density of 639.6 people/km^2 (Al-Shabeeb et al., 2022). Climatologically, Jerash city normally experiences hot, dry summers and temperate to warm, rainy winters due to its Mediterranean climate. The winter months see the most rainfall, often in the form of strong storms that can cause slope instability and flash floods (The Jordan Times, 2020).

GEOLOGICAL SETTING

Jerash clay deposits are part of the Early Cretaceous Kurnub Group of Jordan, as well as the Upper Cretaceous Fuheis Formation. In northern Jordan, the Kurnub Group (KG) is subdivided into three formations, from base to top: Ramel, Jerash, and Bir Fa'as (Amireh and Abed, 1999; Amireh, 2000).

Jerash area is situated roughly 20–25 km north of the Amman–Halabat structure and 20 km east of the Jordan Valley Fault. A portion of the NE-SW Wadi Shu'ayb structure crosses the southern portion of the research region. Monoclinal flexures, faults, and en echelon folds are its constituents. The study area was traversed by the Zarqa River fault in an E-W orientation. Mass movement is motivated and occurs as a result of incentive drainage driven by tectonic phases (Sawariah and Barjous 1993, Abdelhamid 1993).

Over the past few decades, Jerash's land use has changed significantly due to population growth, agricultural development, and urbanization. The three main forms of land cover are

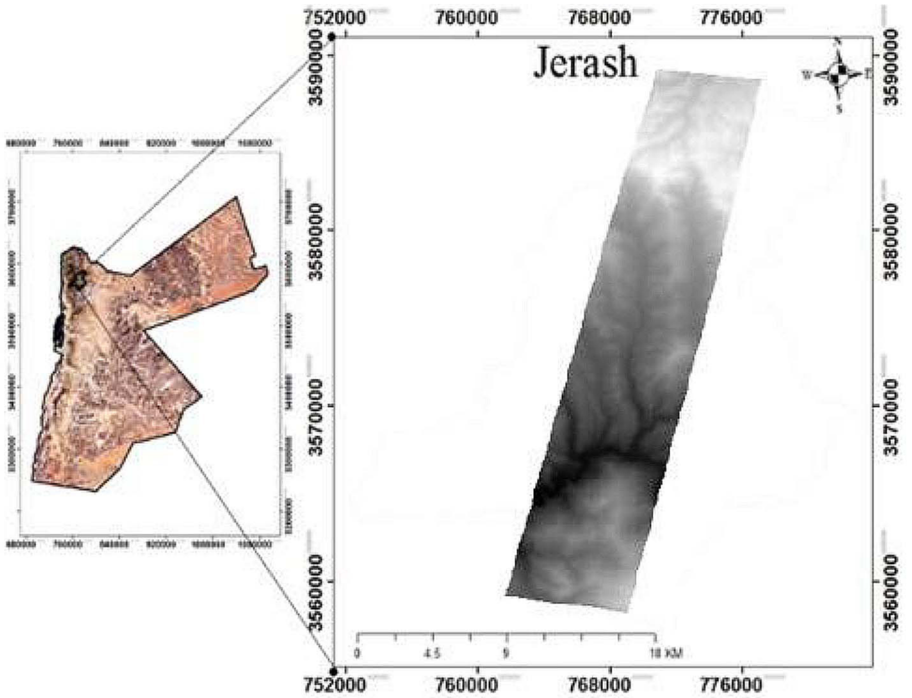

Figure 1. Map of the study area

built-up areas, forests, and agricultural fields; urbanization frequently results in the loss of rangelands and forests (Al-Bakri et al., 2013; Al-Qudah, 2011). Soils in Jerash are mostly clay loam, formed over limestone and colluvial deposits, and categorized primarily as Lithic Xerorthents, which influence hydrological and geotechnical processes (Abu-Awwad, 1998). Recent studies have emphasized the role of soil conditions in local hazards: Alharahsheh et al. (2025) developed a flood forecasting framework for the Jerash Basin by highlighting how soil and land use characteristics affect runoff, while Al Fukaha et al. (2024) investigated the freeze-thaw durability of clayey soils from Jerash, demonstrating the importance of stabilization methods in improving soil performance. These findings demonstrate that soil parameters in Jerash have an important role in hydrological modeling and geotechnical stability.

Jerash has a variety of lithological formations and soil types, along with intense land use and infrastructure near steep slopes, which increase geotechnical risks in the area. Recent research has identified rainfall intensity, slope gradient, lithology, land cover, distance to roads, and hydrological indices like the Stream Power Index and the Normalized Difference Vegetation Index as critical factors influencing landslide susceptibility in Jerash (Al-Najjar et al., 2022).

METHODOLOGY

Criteria affecting the map of landslide susceptibility

The identification of landslide conditioning elements is crucial for attaining high modeling precision. No established guidelines exist regarding the parameters influencing the landslide susceptibility model (Vakhshoori et al., 2019). The conditioning factors of landslides depend on the specific characteristics of the case study, the nature of the landslide occurrence, and the analytical scale employed (Tseng et al., 2015). This study identified 7 conditioning elements for generating landslide susceptibility maps, taking into account the specific characteristics of the study location, the existing literature, and data availability. The selection of the seven factors in this study was not arbitrary, but rather based on precise scientific criteria related to the specific geological and geomorphological characteristics of the Jerash region. It's worth noting that the region is characterized by its unique rocky terrain and topography. Furthermore, using a carefully selected set of factors directly relevant to the region yields more accurate results, unlike selecting factors unsuitable for the local geological context. The study by Saaty and Ozdemir (2003) concluded that it should keep seven numbers or fewer would affect the landslide susceptibility. It appears that Miller's seven plus or minus two is indeed a limit, a channel capacity that affects our ability to process information. The seven parameters include topography, Geology and Soil Factor, Land Cover Factor, and hydrological elements. Data were gathered from different sources as presented in Table 1.

However, topographic factors include elevation, slope, and aspect. Moreover, geology and soil factor include lithology type and soil type. Land cover factor include land use/land cover (LULC). Hydrological factors include average annual rainfall. These criteria were categorized into four groups, distributed as follows:

Topographic factors

These criteria relate to the topography of the area: Slope, Aspect, and Elevation. Terrain conditions directly affect landslide occurrence, particularly the slope gradient and geomorphological setting. Steep and elevated hillslopes, especially areas located along valley edges or dissected ridges, are more susceptible to slope failure due to gravitational forces and reduced material stability (Yalcin, 2008), and hence, slope has been repeatedly employed in landslide susceptibility studies. Slope stability depends on the slope angle; the steeper the slope, the higher the probability of a landslide (Afzal et al., 2022). Figure 2a illustrates the slope map generated from a DEM using ArcGIS 10.8, with slope values ranging between 0° and 46°, separated into five classes: very gentle slope (0–6.7°), gentle slope (6.7–11.2°), moderately steep slope (11.2–16.1°), steep slope (16.1-22.7°), and extremely steep slopes or escarpments (>22.7°). The occurrence of a landslide is exceedingly improbable due to reduced shear stress in the first class. Weights were assigned to each class based on the notion that landslide vulnerability increases with increasing slope steepness (Kanwal et al., 2016). Aspect is another topographic parameter used in landslide susceptibility studies and is also used to determine the direction of slopes face. Aspect features are linked to various factors, including the duration of solar exposure on slopes, moisture retention, vegetation, and climatic conditions (Dai and Lee, 2002). We created the aspect from the DEM data using the GIS aspect analysis tool. It was classified for landslide susceptibility analysis based on geographical aspects (Figure 2b).

Elevation significantly influences landslide incidence by interacting with other regulating elements, including slope gradient, rainfall intensity, geological structure, and vegetation cover (Demirel et al., 2025). In the study area, elevated zones typically experience increased precipitation and possess steeper gradients. Elevated precipitation at higher elevations amplifies surface runoff and subsurface infiltration, diminishing soil shear strength and slope stability, thereby heightening the probability of landslide occurrence. The elevation map was derived from DEM data. The lowest level in the study is 189 m, and the highest level is 1081 m (Figure 2c).

Geology and soil factor

The nature of lithology and soil texture in the area influences the landslide occurrence. A landslide is a geomorphological phenomenon closely linked to the terrain's lithological properties. Diverse lithological units exhibit differing strengths and variable degrees of susceptibility (Yalcin et al. 2011). According to the classification, the Jerash region contained three rock classes: (limestone, dolomitic limestone), (marl, limestone, dolomite), and (sandstone), as shown in Figure 2d. The type of soil can substantially affect the possibility of landslides. Various soil types exhibit distinct characteristics, including density and water-holding capacity (Ray et al. 2010). The soil map is classified into three categories: "Clay", "Silty Clay Loam", and "Silty Clay" as shown in Figure 2f. So, the study area is abundant in clay

Table 1. Data types, characteristics, sources

Data	Source	Characteristics
DEM	United States Geological Survey USGS (freely accessible for download from the USGS website)	30 m spatial resolution
Geology	USGS/ Lithological data (Geological Map of Jordan)	Scale 1:50,000
Soil	Jordanian Ministry of Agriculture	Scale 1:50,000
LULC	USGS	30 m spatial resolution derived from Landsat 8 imagery 2022
Rainfall	Ministry of Water and Irrigation	Scale 1:50,000

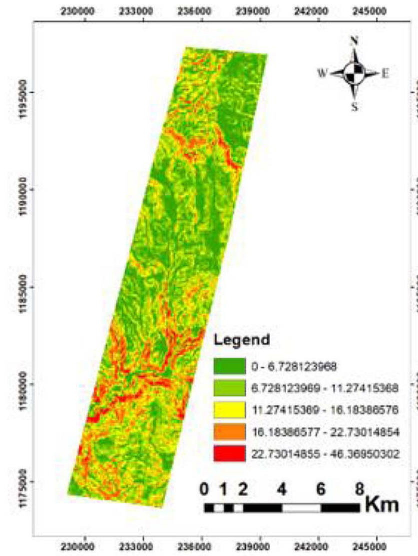

Slope (a)

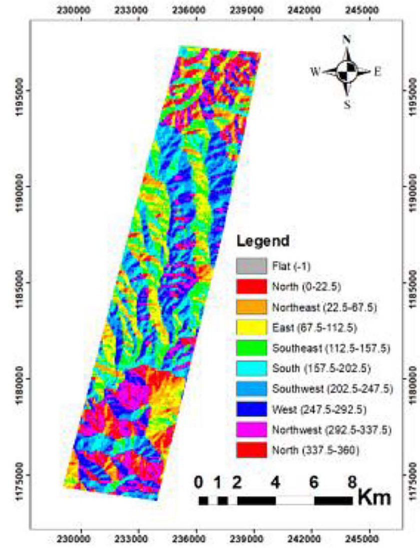

Aspect (b)

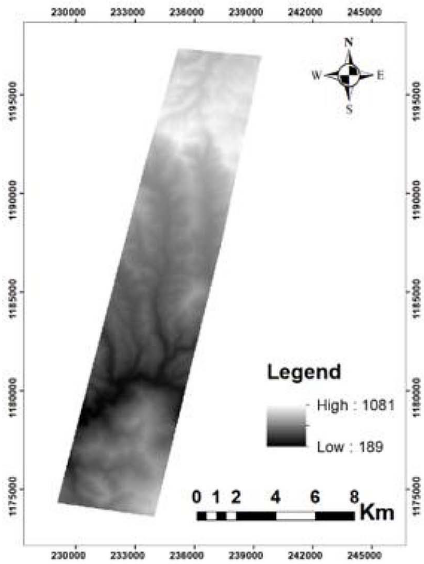

Elevation (c)

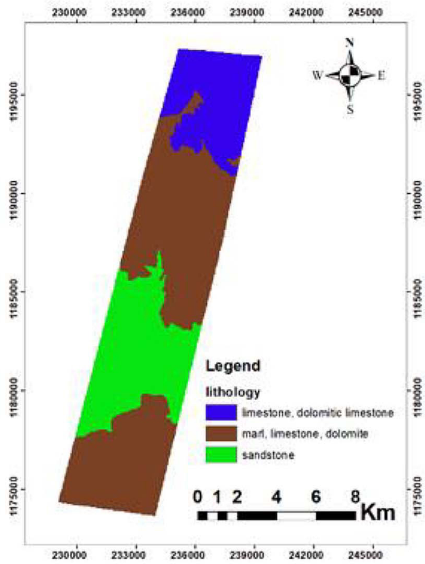

Lithology (d)

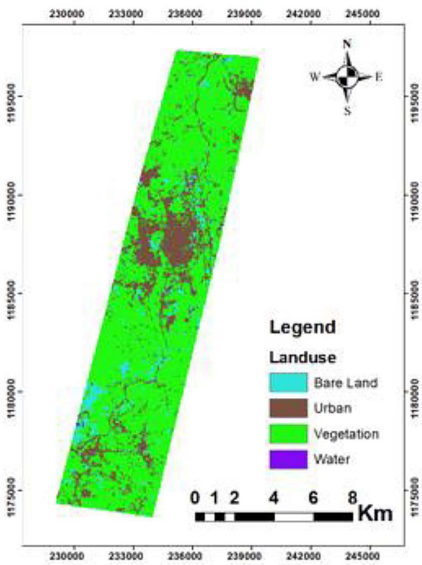

Landuse (e)

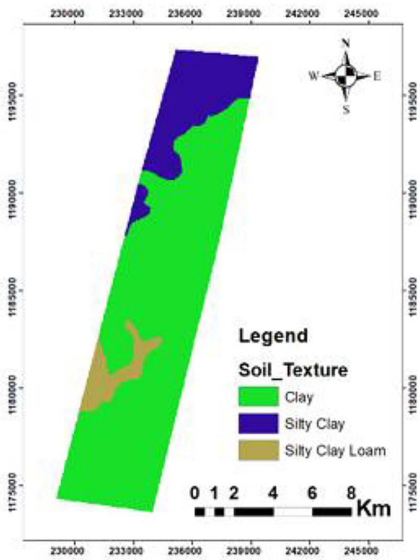

Soil type (f)

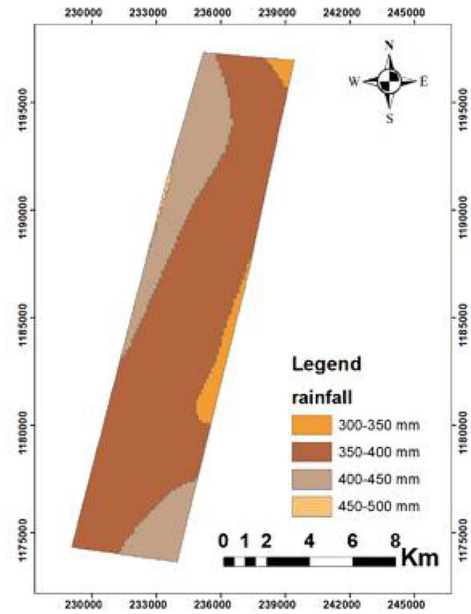

Rainfall (g)

Figure 2. Represent maps of the criteria affecting of Landslide Susceptibility: (a) slope, (b) aspect, (c) elevation, (d) lithology, (e) landuse, (f) soil type, (g) rainfall

soil, which considerably increases slope instability due to its swelling-shrinkage behavior. Upon exposure to water, clay minerals absorb moisture, expand, and reduce shear strength, resulting in decreased slope stability and an increased probability of landslides, particularly on steep inclines (Wang et al., 2024).

Land cover factor

The LULC markedly affects landslide risk, as vegetation enhances slope stability by increasing soil cohesion and mitigating surface erosion through root reinforcement. Conversely, deforested or urbanized regions demonstrate compromised soil structure and reduced root anchorage, heightening the risk of slope failure, especially during heavy rainfall occurrences (Pradhan and Lee, 2010). In this study, the LULC map was categorized into four primary classes: Bare Land, Urban, Vegetation, and Water, as shown in Figure 2e.

Hydrological factors

Precipitation serves as the principal natural trigger for landslides, as it enhances the movement of slope materials through increase the soil moisture content and diminish the soil strength. The impact of precipitation is additionally influenced by geographical differences in terrain and vegetation cover, which alter infiltration rates and surface runoff dynamics. (Cheng et al., 2025). The research area exhibits high fluctuations in the annual precipitation rate. The data were categorized into four intervals: 300–350, 350–400, 400–450, and 450–500 mm/year (Figure 2g). Table 2 represents the class, rating, and reference for each criterion.

For our analysis of landslide susceptibility, we relied on a detailed landslide inventory to create a strong base. The main source of data for this inventory was Diabat et al. (2022), who pinpointed nine major landslide stations in the study area. These recorded sites were rechecked and expanded with our field records to ensure the data are up to date. The locations and susceptibility categories of these stations are shown in Table 3. Combining documented data with our own field data yields crucial ground-truthing observations indispensable for effective susceptibility model calibration and validation.

The AHP method

The AHP is a recognized methodology for MCDM employed to ascertain the weight of different factors. It is a mathematical approach that integrates qualitative and quantitative components, together with individual or collective subjective assessments for sustainability (Yamusa et al., 2022). One of the major advantages of AHP is that it enables the active involvement of decision-makers and domain experts familiar with slope stability and geological conditions (Chen, 2016). Numerous studies have applied AHP to generate scalable susceptibility maps that assess landslide risk (Yalcin, 2008; Pradhan & Lee, 2010). The workflow typically begins by identifying the key conditioning factors affecting landslide occurrence, which are determined through an extensive review of scientific studies on the topic over the past decade. Or by creating a survey and distributing it to several experts who have comprehensive knowledge of the study area. This study did not rely on the traditional AHP Pairwise Comparison matrix, but rather adopted the methodology based on weights derived from previous studies, where the main and similar factors were identified and their ready-made weights were adopted as a scientific alternative approved in AHP research to determine the importance of each factor, due to the similarity of the characteristics between the

Table 2. Represent class, rating and reference of each criterion

Criteria	Class	Rating	Weight	Reference
Elevation (m)	<400	1	8.8	Al-Sababhah, 2022
	401–600	2		
	601–800	3		
	801–1000	4		
	>1000	5		
Slope (°)	0–15	1	22.2	Ibrahim, et al., 2025
	15–25	2		
	25–35	3		
	35–50	4		
	50–90	5		
Aspect	0–67° (NE)	1	8	Liu et al., 2024 Alharbi et al. (2024)
	68–139° (NE–SE)	2		
	140–208° (SE–SW)	3		
	209–283° (SW–NW)	4		
	284–360° (NW)	5		
Lithology (Class)	Clay, Silt	3	16	Awawdeh et al., 2018 El Jazouli et al., 2019
	Basalt	2		
	Limestone	5		
	Dolomite	3		
	Sandstone	2		
Soil Texture (Class)	Sandy loam	1	18	Awawdeh et al., 2018 Tešić et al., 2020
	Loamy	2		
	Silty clay loam	3		
	Silty clay	4		
	Clay	5		
LULC (Class)	Water bodies	1	13	Ibrahim et al., 2025
	Vegetation	2		
	Rangland, crops	3		
	Bare ground	4		
	Built area, rock area	5		
Rainfall (mm)	<50	1	14	Al-Sababhah, 2022
	51–100	2		
	101–200	3		
	201–400	4		
	>401	5		

current study area and some of the areas previously studied in the literature, and to avoid personal bias in pairwise comparisons. The relative weights were then used to construct the pairwise comparison matrix following Saaty's method. The comparison follows a scale from one to nine, where nine indicates the highest importance, and one indicates the lowest (Saaty, 1990).

After determining the final weights for each of the seven criteria based on a comprehensive review of previous studies, the values were normalized so that their sum equals 1.0. Each criterion map was subsequently reclassified using the Reclassify tool in ArcGIS 10.8 (Spatial Analyst Tools), with values assigned on a scale from 1 to 5 based on their relative impact on landslide susceptibility, where 1 denotes very low susceptibility, and 5 denotes very high susceptibility. The classification thresholds for each class were defined manually based on expert judgment and the physical characteristics of each factor, rather than automated statistical methods. The final landslide

Table 3. Verified landslide stations and susceptibility classification (Based on the landslide inventory by Diabat et al., 2022)

Station ID	Location description	Coordinates (Lat/Long)	Susceptibility class
Station 1	Southern	32° 13 / 35° 53	Low
Station 2	Jerash-Amman Hwy	32° 13 / 35° 53	Moderate
Station 3	Jerash-Amman Hwy	32° 12 / 35° 51	Moderate
Station 4	Northern	32° 11 / 35° 51	High
Station 5	Northern	32° 11.5 / 35° 51.6	High
Station 6	Central	32° 06.95 / 35° 51.26	High
Station 7	Central	32° 13.7 / 35° 53.6	High
Station 8	Northern	32° 12.34 / 35° 52.25	High to moderate
Station 9	Southern	32° 9.7 / 35° 50.8	Moderate

susceptibility map was then generated using the Raster Calculator tool in ArcGIS 10.8, by multiplying each reclassified raster by its corresponding normalized weight and summing the resulting layers, following the equation:

$$\begin{aligned} LSI = {} & (0.088 \times E) + (0.222 \times S) + \\ & + (0.080 \times A) + (0.160 \times Li) + \\ & + (0.180 \times ST) + (0.140 \times R) + \\ & + (0.130 \times LULC) \end{aligned} \quad (1)$$

where: *LSI* – the landslide susceptibility index, *E*, *S*, *A*, *Li*, *ST*, *R*, and *LU* – the reclassified raster values for elevation, slope, aspect, lithology, soil texture, rainfall, and land use/land cover, respectively.

The consistency ratio (CR) is determined by using the random consistency index scale (RI), which depends on the number of criteria (Table 4). The matrix's consistency value is deemed acceptable if the CR is below 0.1 (Senapati and Das, 2022). Nonetheless, having a CR above 0.1 (10%) necessitates an examination of the decision-makers' choice matrix (Yamusa et al., 2022). The following equations were used in the study:

$$\lambda max = \frac{1}{n}\sum_{i=1}^{n}\frac{(A.w)i}{wi} \quad (2)$$

where: *λmax* – the principal eigenvalue of the pairwise comparison matrix, *n* – the number of criteria, *A* – the pairwise comparison matrix, w - the priority weight vector.

$$CI = \frac{\lambda max - n}{n-1} \quad (3)$$

where: *CI* – consistency index, *n* – the number of criteria.

$$CR = \frac{CI}{RI} \quad (4)$$

where: *CR* – consistency ratio, *CI* – consistency index, *RCI* – random consistency index.

RESULTS AND DISCUSSION

One of our research aims was to identify the primary factors that precipitate landslides using the AHP. Based on expert opinions, previous study results showed that slope received the highest weightage of 22.2, followed by soil texture (18) and geology/lithology (16). However, the pairwise comparison matrix was created using the relative weights obtained from previous research. The matrix values indicate the interrelationships among the seven elements affecting landslide susceptibility in the Jerash region. The CI was 0, and CR was 0.05, signifying flawless mathematical consistency. This outcome is attributed to the matrix's derivation from weights reported in the scientific literature, thereby affirming the credibility of the criteria weights used in this study. Table 5 represents the pairwise comparison matrix and the results for checking the consistency of the AHP model.

Each zone depicted in the maps of Figure 2 was evaluated based on landslide susceptibility, as illustrated in Figure 3. In selecting the criteria depicted in Figures 2 and 3, a comprehensive examination of all pertinent institutions' open databases was conducted, considering significant factors that may influence landslide susceptibility. Consequently, a comprehensive, more nuanced investigation into the region's landslide vulnerability was undertaken.

Table 4. Average random consistency index (Saaty, 1990)

N	1	2	3	4	5	6	7	8	9	10	11	12
Random consistency index	0	0	0.52	0.89	1.11	1.25	1.35	1.40	1.45	1.49	1.51	1.48

The slope aspect affects landslide vulnerability in the Jerash area by influencing moisture retention and microclimatic conditions. North- and north-east-facing slopes are more susceptible due to decreased solar radiation and prolonged soil wetness, whereas south-facing slopes are more stable, as shown in Figure 3b (Guzzetti et al., 1999; Yilmaz, 2009; Ayalew and Yamagishi, 2005). Elevation is a key factor controlling landslide susceptibility in the Jerash area, with high-altitude plateaus showing the highest susceptibility (Figure 3c). Higher elevations increase precipitation and soil moisture, reducing slope stability and increasing the risk of landslides, as confirmed by GIS–AHP modeling in northern Jordan (Al Sababhah, 2022).

The slope aspect affects landslide vulnerability in the Jerash area by influencing moisture retention and microclimatic conditions. North- and north-east-facing slopes are more susceptible due to decreased solar radiation and prolonged soil wetness, whereas south-facing slopes are more stable as shown in Figure 3b (Guzzetti et al., 1999; Yilmaz, 2009; Ayalew and Yamagishi, 2005). E Elevation is a key factor controlling landslide susceptibility in the Jerash area, with high-altitude plateaus showing the highest susceptibility (Figure 3c). Higher elevations increase precipitation and soil moisture, reducing slope stability and promoting landslides, as confirmed by GIS–AHP modeling in northern Jordan (Al-Sababhah, 2022).

Lithology is a primary determinant of landslide occurrence in the Jerash region (Figure 3d). Marl formations exhibit significant landslide susceptibility owing to their clay-rich composition, diminished shear strength, and marked loss of mechanical stability under saturated conditions, as evidenced by their prevalence in high-susceptibility categories (Selby, 1993; Bell, 2007). Limestone and dolomite formations exhibit significant landslide susceptibility due to the extensively faulted and fractured geological conditions of the Jerash region, where structural discontinuities and karstic features diminish rock mass strength and foster instability on steep slopes (Abed and Al-Khouri, 2006; Cruden and Varnes, 1996). Sandstone formations exacerbate landslide occurrence, especially in areas with weak cementation and fine-grained materials that diminish intergranular cohesion and slope stability (Bell, 2007). The spatial distribution of susceptibility classes from the AHP-weighted GIS model indicates that these lithological units are primarily associated with areas of elevated landslide risk, highlighting the direct impact of rock type on slope instability in the study region (Chen et al., 2016).

Land use has a substantial impact on landslide vulnerability in the Jerash area (Figure 3e), with more landslides occurring in areas with intensive agricultural and urban land uses. This pattern emerges as a result of decreasing plant cover and increasing human disturbance, which increases surface runoff and weakens soil cohesion, contributing to slope instability. The landslide susceptibility mapping study for northern Jordan (including the Jerash-Amman corridor) discovered that both agricultural and urban land

Table 5. Pairwise comparison matrix derived from literature-based weights and consistency check (λmax, CI, RI, CR)

Criterion	Elevation	Slope	Aspect	Lithology	Soil texture	Rainfall	LULC	Weight
Elevation	1.000	0.396	1.100	0.550	0.489	0.677	0.629	8.8%
Slope	2.523	1.000	2.775	1.387	1.233	1.708	1.586	22.2%
Aspect	0.909	0.360	1.000	0.500	0.444	0.615	0.571	8.0%
Lithology	1.818	0.721	2.000	1.000	0.889	1.231	1.143	16.0%
Soil Texture	2.045	0.811	2.250	1.125	1.000	1.385	1.286	18.0%
Rainfall	1.591	0.631	1.750	0.875	0.778	1.000	1.077	14.0%
LULC	1.477	0.586	1.625	0.813	0.722	0.929	1.000	13.0%

λmax	RI (n=7)	CI	CR	Consistency check
7.00	1.35	0.00	0.05	CR < 0.1 (Yes)

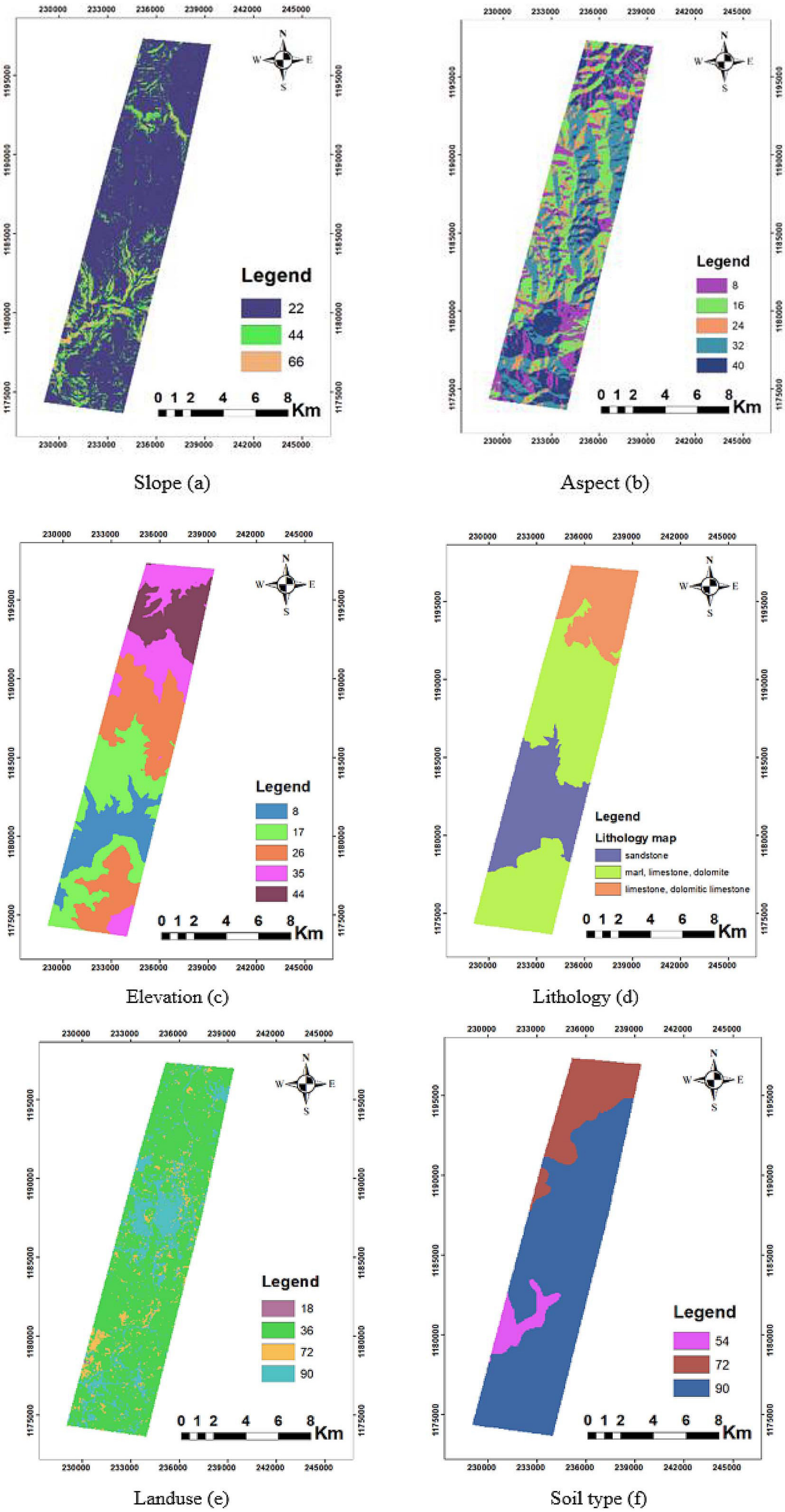

Figure 3. Landslide susceptibility factors after AHP method: (a) slope, (b) aspect, (c) elevation, (d) lithology, (e) landuse, (f) soil type

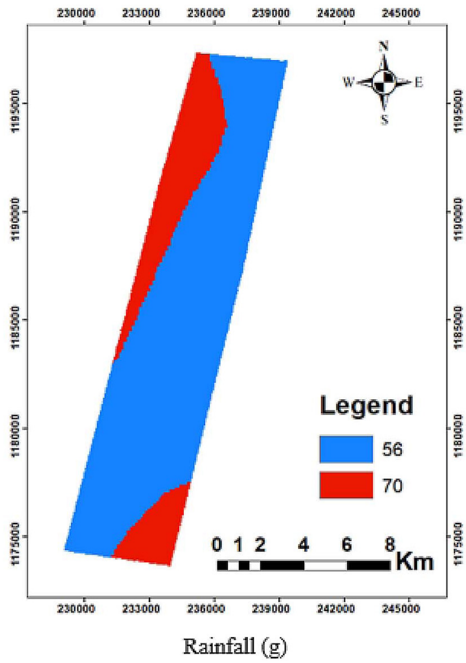

Figure 3. Landslide susceptibility factors after AHP method: (g) rainfall)

use areas are prominently located within high and very high susceptibility zones, confirming the importance of land use as a conditioning factor in landslide occurrence (Awawdeh et al., 2018).

Landslides are more likely in the Jerash area due to the prevalence of fine-textured and clay-rich soils, which encourage water retention and reduce shear strength in wet conditions. GIS-AHP landslide susceptibility mapping in Jerash northern highlands reveals that clay-dominant soils correlate with higher susceptibility zones, showing that soil type is a major conditioning factor for slope instability (Figure 3f) (Awawdeh et al., 2018). Last important criterion that triggers landslides is precipitation. Results revealed that all parts receive rainfall exceeding 300 mm/year, which is clear evidence of the area's high risk of landslides. Seeping Water toward the ground as a result of precipitation may trigger landslides. Thus, the northwest and southeastern regions were scored at high level (Figure 3g). The clay soils were evaluated also as highly sensitive. Figure 4 shows that the landslide susceptibility is colored in three different degrees: low susceptible, moderate susceptible, and high susceptible. The integrated landslide susceptibility map indicates that moderate and high susceptibility zones are concentrated in the central, northern, and southeastern sections of the study area, which are characterized by steep slopes, weak lithology, intensive agriculture, and rapid erosion. To verify the results' accuracy, four points in the study area within the Moderate and High ranges were matched with previous studies and recorded landslide areas. Point 1 is located 200 meters north of the Zarqa River at the coordinate of 32° 13. 375'N and 35° 53.536' E. Point 2 is located to the northeast of Point 1 along Jerash-Amman Highway at 32° 13.741' N and 35° 53.816' E. Point 3 is located south of Zarqa River and opposite King Talal Dam, 10 km south of Jerash city. It is coordinated at 32° 12. 048'N and 35° 51.932' E. Point 4 is located along the Jerash-Amman Highway, about 15 km south of Jerash. It is coordinated at 32° 11. 713' N and 35° 51.878' E, as illustrated in Figure 4, thereby demonstrating robust predictive capacity and reliability for hazard assessment.

Model validation

To assess which AHP-GIS model predicted the best landslide susceptibility, the spatial validation of the generated susceptibility map was carried out using a landslide inventory comprising only nine landslide locations documented and identified by Diabat et al. (2022). The validation analysis mathematically measured how well the model's sus zones correspond to the actual distribution of landslides. The statistical distribution of these nine landslide location stations showed a very good spatial correlation between the 'high'

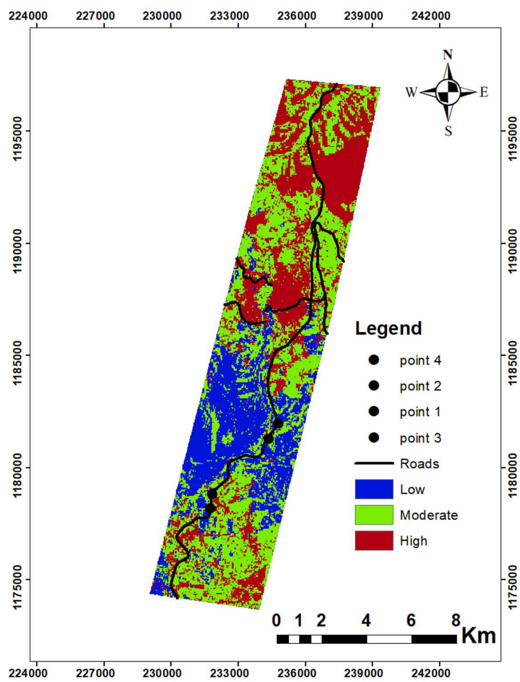

Figure 4. Landslide susceptibility map

Table 6. Distribution of the documented landslide stations within the susceptibility zones

Susceptibility zone	Very low	Low	Moderate	High	Very high
Percentage of landslide stations (%)	0	11.1	33.3	44.5	11.1

and 'very high' susceptibility zones and the inventory landslides. The distribution of different susceptibility classes is presented in Table 6.

The analysis indicates that about 55.6% of the stationed landslides are well captured in the (high and very high (susceptibility zones, while the remaining stations fall into the moderate zone, and none are in the very low zone. This strong spatial correlation demonstrates the model's trustworthiness and its ability to locate landslide-prone areas. These findings verify that the chosen conditioning factors and the AHP weighting method are appropriate for regional hazard assessment and proactive land-use planning in the Jerash area.

CONCLUSIONS

Landslides constitute a substantial natural danger impacting the viability of ecosystems and human habitats. This study evaluated landslide susceptibility in the Jerash region of Jordan and identified seven parameters that influence it. The landslide susceptibility map was generated. The findings indicate that the center, northern, and southeastern regions of the research area exhibit moderate to high landslide sensitivity. Slope, soil texture, and lithology were identified as the most significant elements in precipitating landslide events. The landslide susceptibility map demonstrated high predictive accuracy, indicating the robustness and reliability of the modeling methodology.

This study's findings establish a scientific foundation for land-use planning and landslide risk control in the area examined. The produced susceptibility map facilitates the identification of high-risk areas and supports informed decision-making to prioritize mitigation strategies. These findings can inform slope stabilization initiatives, govern land-use practices, and facilitate safer infrastructure planning, ultimately mitigating landslide-related consequences and bolstering long-term resilience and sustainable development.

Acknowledgments

The authors would like to express their sincere gratitude to all individuals who contributed to the completion of this study. Special appreciation is extended to Ibn Tufail University (Morocco) and Al al-Bayt University (Jordan) for their valuable support, collaboration, and provision of the necessary facilities that made this research possible.

REFERENCES

1. Abdelhamid, G. (1993). Geological map of Jarash scale 1:50,000, sheet no. 3154-I. *Natural Resources Authority, Amman, Jordan.*
2. Abed, A., Al-Kharabsheh, A., Shatnawi, M. (2022). Spatial mapping of landslide susceptibility in Jerash Governorate, northern Jordan. *Georisk: Assessment and Management of Risk for Engineered Systems and Geohazards, 16*(4), 421–438. https://doi.org/10.1080/19475705.2022.2112096
3. Abed, A.M., Al-Khouri, A.M. (2006). Geological evolution of the Ajlun area, northern Jordan. *Jordan Journal of Earth and Environmental Sciences*.
4. Abu-Awwad, A. M. (1998). Water infiltration and redistribution within soils affected by Jordan's climate. *Arid Soil Research and Rehabilitation, 12*(3), 233–242. https://doi.org/10.1080/15324989809381515
5. Ahmed, M. F., Rogers, J. D., Ismail, E. H. (2014). *A regional level preliminary landslide susceptibility study of the upper Indus river basin. European Journal of Remote Sensing, 47*(1), 343–373. https://doi.org/10.5721/EuJRS20144721
6. Al Fukaha, R., Shaqour, F., Ismeik, M. (2024). Freeze–thaw durability of clayey soils stabilized by alkaline-activated kaolin and recycled cement kiln dust. *Results in Engineering, 24*, 103199. https://doi.org/10.1016/j.rineng.2024.103199
7. Al-Bakri, J., Salahat, M., Suleiman, A., Suifan, M., Hamdan, M. R., Khresat, S., Kandakji, T. (2013). Impact of climate and land use changes on water and food security in Jordan: Implications for transcending "the tragedy of the commons." *Sustainability, 5*(2), 724–748. https://doi.org/10.3390/su5020724
8. Alharahsheh, M., Al Fukaha, R., Ibrahim, M., Chakiri, S. (2025). Developing a scalable framework for accurate flood forecasting in arid regions: A case study of the Jerash Basin, Jordan. *Ecological Engineering & Environmental Technology, 26*(4), 347–356. https://doi.org/10.12912/27197050/201999
9. Alharbi, T., El-Sorogy, A. S., Al-Kahtany, K., Salem, Y., Rikan, N. (2024). *Landslide susceptibility assessment using the analytic hierarchy process (AHP):*

A case study of Al Figrah Road, Al-Madinah, Saudi Arabia. Preprints. https://doi.org/10.20944/preprints202410.1125.v1.

10. Al-Najjar, H., Al-Rawabdeh, A., Kadi, R. (2022). GIS-based assessment of rainfall-induced landslides in northern Jordan. *Environmental Earth Sciences, 81*(6), 1–15. https://doi.org/10.1007/s12665-022-10345-1
11. Al-Qudah, K. A. (2011). Land cover change in Bourma sub-district/Jerash governorate using GIS and remote sensing techniques. *Jordan Journal of Agricultural Sciences, 7*(1), 1–15.
12. Al-Rawabdeh, A., Awawdeh, M., Al Quraan, H., Jaradat, R. (2023). Modeling landslides hazard along Amman–Jerash–Irbid Highway, Jordan by integrating open street map (OSM) and weighted linear combination (WLC) techniques. *Modeling Earth Systems and Environment, 10*(2), 1–19. https://doi.org/10.1007/s40808-023-01910-3
13. Al-Sababhah, N. M. A. (2022). Development of landslide susceptibility mapping using GIS Modeling in Jordan's Northern highlands. *Environment and Ecology Research*, *10*(6), 701–727.
14. Al-Shabeeb, A. R., Al-Fugara, A., Khedher, K. M., Mabdeh, A. N., Al-Adamat, R. (2022). Spatial mapping of landslide susceptibility in Jerash governorate of Jordan using genetic algorithm-based wrapper feature selection and bagging-based ensemble model. *Geomatics, Natural Hazards and Risk*, *13*(1), 2252–2282. https://doi.org/10.1080/19475705.2022.2112096
15. Althuwaynee, O. F., Pradhan, B. (2017). *Semi-quantitative landslide risk assessment using GIS-based exposure analysis in Kuala Lumpur City. Geomatics, Natural Hazards and Risk, 8*(2), 706–732. https://doi.org/10.1080/19475705.2016.1255670
16. Amireh, B. S. (2000). Surface and subsurface occurrences of the new Infracambrian Umm Ghaddah Formation in Jordan: Tectonic implications. *Dirasat, Pure Sciences, University of Jordan, 27*, 143–168.
17. Amireh, B. S., Abed, A. M. (1999). Depositional environments of the Kurnub Group (Early Cretaceous) in northern Jordan. *Journal of African Earth Sciences, 29*(4), 449–468.
18. Awawdeh, M. M., ElMughrabi, M. A., Atallah, M. Y. (2018). Landslide susceptibility mapping using GIS and weighted overlay method: A case study from North Jordan. *Environmental Earth Sciences, 77*(21), 732. https://doi.org/10.1007/s12665-018-7910-8.
19. Ayalew, L., Yamagishi, H. (2005). The application of GIS-based logistic regression for landslide susceptibility mapping. *Geomorphology*, *65*, 15–31. https://doi.org/10.1016/j.geomorph.2004.06.010
20. Ayalew, L., Yamagishi, H., Marui, H., Kanno, T. (2005). *Landslides in Sado Island of Japan: Part II. GIS-based susceptibility mapping with comparisons of results from two methods and verifications. Engineering Geology, 81*(4), 432–445. https://doi.org/10.1016/j.enggeo.2005.08.004
21. Aydın, M. C., Sevgi Birincioğlu, E., Büyüksaraç, A. (2022). *Landslide susceptibility mapping in Bitlis Province using GIS-based AHP method. Türk Uzaktan Algılama ve CBS Dergisi*, *3*(2), 160–171. https://doi.org/10.48123/rsgis.1119723
22. Barredo, J. I., Benavides, A., Hervás, J., van Westen, C. J. (2000). *Comparing heuristic landslide hazard assessment techniques using GIS in the Tirajana basin, Gran Canaria Island, Spain. International Journal of Applied Earth Observation and Geoinformation, 2*(1), 9–23. https://doi.org/10.1016/S0303-2434(00)85022-9
23. Bell, F.G. (2007). *Engineering Geology (2nd ed.)*. Elsevier.
24. Chen, W., Li, W., Chai, H., Hou, E., Li, X., Ding, X. (2016). GIS-based landslide susceptibility mapping using the analytical hierarchy process (AHP) and certainty factor (CF) models for the Baozhong region of Baoji City, China. *Environmental Earth Sciences, 75*(1), Article 63. https://doi.org/10.1007/s12665-015-4795-7
25. Cheng, C., Li, Y., Zhu, D., Liu, Y., Wu, Y., Lin, D., Guo, H. (2025). *Rain-induced shallow landslide susceptibility under extreme precipitation conditions. Applied Sciences, 15*(11), 6241. https://doi.org/10.3390/app15116241
26. Cruden, D.M., Varnes, D.J. (1996). *Landslide types and processes.* In A.K. Turner & R.L. Schuster (Eds.), Landslides: Investigation and Mitigation (Special Report 247, pp. 36–75). Transportation Research Board.
27. Dai, F.C., Lee, C.F. (2002). Landslide characteristics and slope instability modeling. *Engineering Geology, 65*, 1–18. https://doi.org/10.1016/S0013-7952(01)00113-3
28. Demirel, B., Yıldırım, E., Can, E. (2025). *GIS-based landslide susceptibility mapping using AHP, FMEA, and Pareto systematic analysis in central Yalova, Türkiye. Engineering Science and Technology, an International Journal, 64*, Article 102013. https://doi.org/10.1016/j.jestch.2025.102013
29. Diabat, A., Ibrahim, M., Al-Hawareen, Y. (2022). Kinematic Analysis of Landslides: A Case Study Along Jerash-Amman Highway, Jordan. *Jordan Journal of Earth and Environmental Sciences, 13*(3), 177–189.
30. El Jazouli, A., Barakat, A., Khellouk, R. (2019). *GIS-multicriteria evaluation using AHP for landslide susceptibility mapping in Oum Er Rbia high basin (Morocco). Geoenvironmental Disasters, 6*, Article 3. https://doi.org/10.1186/s40677-019-0119-7
31. Guzzetti, F., Carrara, A., Cardinali, M., Reichenbach, P. (1999). Landslide hazard evaluation: a review of current techniques. *Geomorphology, 31*, 181–216. https://doi.org/10.1016/S0169-555X(99)00078-1
32. Ibrahim, I. L., Hashim, N., Othman, A. N., Talib, N., Shaharuddin, S. (2025). Landslide susceptibility assessment using analytical hierarchy process (AHP)

in Hulu Selangor. *Revue Internationale de Geomatique*, *34*(1), 915–937.

33. Kanwal, S., Atif, S., Shafiq, M. (2017). *GIS based landslide susceptibility mapping of northern areas of Pakistan, a case study of Shigar and Shyok Basins. Geomatics, Natural Hazards and Risk, 8*(2), 348–366. https://doi.org/10.1080/19475705.2016.1220023
34. Kumar, R., Anbalagan, R. (2016*). Landslide susceptibility mapping using analytical hierarchy process (AHP) in Tehri reservoir rim region, Uttarakhand, India. Journal of the Geological Society of India, 87*(3), 271–286. https://doi.org/10.1007/s12594-016-0395-8
35. Liu, X., Shao, S., Shao, S. (2024). *Landslide susceptibility zonation using the analytical hierarchy process (AHP) in the Great Xi'an Region, China. Scientific Reports, 14*, Article 53630. https://doi.org/10.1038/s41598-024-53630-y
36. Malczewski, J. (1999). *GIS and multicriteria decision analysis*. John Wiley & Sons, Inc.
37. Moradi, M., Bazyar, M. H., Mohammadi, Z. (2012). *GIS-based landslide susceptibility mapping by AHP method, A case study, Dena City, Iran. Journal of Basic and Applied Scientific Research*, *2*(7), 6715–6723.
38. Noorollahi, Y., Sadeghi, S., Yousefi, H., Nohegar, A. (2018). *Landslide modelling and susceptibility mapping using AHP and fuzzy approaches. International Journal of Hydrology, 2*(2), 142–153. https://doi.org/10.15406/ijh.2018.02.00063
39. Pradhan, B., Lee, S. (2010). *Landslide susceptibility assessment and factor effect analysis: backpropagation artificial neural network and frequency ratio approach. Environmental Modelling & Software, 25*(6), 747–759. https://doi.org/10.1016/j.envsoft.2009.10.016
40. Saaty T. L. (1990) How to make a decision: the analytic hierarchy process. *European Journal of Operational Research 48*(1), 9–26. https://doi.org/10.1016/0377-2217(90)90057-i.
41. Saaty, T. L. (1977). *A scaling method for priorities in hierarchical structures. Journal of Mathematical Psychology, 15*(3), 234–281. https://doi.org/10.1016/0022-2496(77)90033-5
42. Saaty, T. L., Ozdemir, M. S. (2003). Why the magic number seven plus or minus two. *Mathematical and Computer Modelling, 38*(3–4), 233–244. https://doi.org/10.1016/S0895-7177(03)90083-5
43. Sawariah, A., Barjous, M. (1993). Geological map of Suwaylih, scale 1:50,000, sheet no. 3154-II. *Natural Resources Authority, Amman, Jordan.*
44. Selby, M.J. (1993). *Hillslope Materials and Processes.* Oxford University Press.
45. Senapati U., Das T. K. (2022) Gis-based comparative assessment of ground water potential zone using MIF and AHP techniques in cooch Behar district, west Bengal. *Applied Water Science 12*(3). https://doi.org/10.1007/s13201-021-01509-y.
46. Shahabi, H., Hashim, M., Ahmad, B. B. (2015). *Remote sensing and GIS-based landslide susceptibility mapping using frequency ratio, logistic regression, and fuzzy logic methods at the central Zab basin, Iran. Environmental Earth Sciences, 73*(12), 8647–8668. https://doi.org/10.1007/s12665-015-4028-0
47. Singh, M., Khajuria, V., Singh, S., Singh, K. (2024). Landslide susceptibility evaluation in the Beas River Basin of the north-western Himalaya: A geospatial analysis employing the analytical hierarchy process (AHP) method. *Science of the Total Environment, 912*, 169065. https://doi.org/10.1016/j.scitotenv.2024.169065.
48. Tešić, D., Đorđević, J., Hölbling, D., Đorđević, T., Blagojević, D., Tomić, N., Lukić, A. (2020). Landslide susceptibility mapping using AHP and GIS weighted overlay method: a case study from Ljig, Serbia. *Serbian Journal of Geosciences*, *6*(1), 9–21.
49. The Jordan Times. (2020, March 12). *Jerash authorities tackle landslides, damage caused by rainfall*. Retrieved from https://jordantimes.com
50. Tseng, C. M., Lin, C. W., Hsieh, W. D. (2015). Landslide susceptibility analysis by means of event-based multi-temporal landslide inventories. *Natural Hazards and Earth System Sciences Discussions, 3*, 1137–1173.
51. Vakhshoori, V., Pourghasemi, H. R., Zare, M., Blaschke, T. (2019). Landslide susceptibility mapping using GIS-based data mining algorithms. *Water, 11*, 2292.
52. Vargas, L. G. (1990). *An overview of the analytic hierarchy process and its applications. European Journal of Operational Research, 48*(1), 2–8. https://doi.org/10.1016/0377-2217(90)90056-H
53. Wang, Q., Zhang, W., Pradhan, B. (2025). Transferability of machine learning models for landslide susceptibility mapping in data-scarce regions. *Gondwana Research, 126*, 180–195. https://doi.org/10.1016/j.gr.2025.01.002
54. Yalcin, A. (2008). *GIS-based landslide susceptibility mapping using analytical hierarchy process and bivariate statistics in Ardesen (Turkey): Comparisons of results and confirmations. Catena, 72*(1), 1–12. https://doi.org/10.1016/j.catena.2007.01.003
55. Yamusa I. B., Ismail M. S., Tella A. (2022). Highway proneness appraisal to landslides along taiping to Ipoh segment Malaysia, using MCDM and GIS techniques. *Sustainability (Switzerland) 14*(15). https://doi.org/10.3390/su14159096.
56. Yilmaz, I. (2009). Landslide susceptibility mapping using frequency ratio, logistic regression and GIS. *Engineering Geology*, *104*, 55–63. https://doi.org/10.1016/j.enggeo.2008.08.003